# Ovarian Steroids Increase PSD-95 Expression and Dendritic Spines in the Dorsal Raphe of Ovariectomized Macaques

**Heidi M. Rivera**[a] and **Cynthia L. Bethea**[a,b,c,d]

[a]Division of Reproductive Sciences, Oregon National Primate Research Center, Beaverton, OR 97006

[b]Division of Neuroscience, Oregon National Primate Research Center, Beaverton, OR 97006

[c]Department of Behavioral Neuroscience, Oregon Health and Science University, Portland, OR 97201

[d]Department of Obstetrics and Gynecology, Oregon Health and Science University, Portland, OR 97201

## Abstract

Estradiol (E) and progesterone (P) promote spinogenesis in several brain areas. Intracellular signaling cascades that promote spinogenesis involve RhoGTPases, glutamate signaling and synapse assembly. We found that in serotonin neurons, E±P administration increases (a) gene and protein expression of RhoGTPases, (b) gene expression of glutamate receptors (c) gene expression of pivotal synapse assembly proteins. Therefore, in this study we determined whether structural changes in dendritic spines in the dorsal raphe follow the observed changes in gene and protein expression. Dendritic spines were examined with immunogold silver staining of a spine marker protein, postsynaptic density-95 (PSD-95) and with Golgi staining. In the PSD-95 study, adult Ovx monkeys received placebo, E, P, or E+P for 1 month (n=3/group). Sections were immunostained for PSD-95 and the number of PSD-95-positive puncta was determined with stereology. E, P and E+P treatment significantly increased the total number of PSD-95-positive puncta (ANOVA, *P*=0.04). In the Golgi study, adult Ovx monkeys received placebo, E or E+P for 1 month (n=3–4) and the midbrain was Golgi-stained. A total of 80 neurons were analyzed with Neurolucida software. There was a significant difference in spine density that depended on branch order (two-way ANOVA). E+P treatment significantly increased spine density in higher-order (3–5°) dendritic branches relative to Ovx group (Bonferroni, P<0.05). In summary, E+P leads to the elaboration of dendritic spines on dorsal raphe neurons. The ability of E to induce PSD-95, but not actual spines, suggests either a sampling or time lag issue. Increased spinogenesis on serotonin dendrites would facilitate excitatory glutamatergic input and, in turn, increase serotonin neurotransmission throughout the brain.

## Keywords

dendritic spines; estradiol; golgi; progesterone; serotonin

---

## Introduction

The serotonin system has been strongly implicated as a target in the treatment of affective disorders, and it has widespread projections throughout the brain that support numerous higher order neural functions (Ressler and Nemeroff, 2000). In humans, a number of studies indicate that the loss of estradiol (E) and progesterone (P), either induced with complete hysterectomy or gradually through menopause, will negatively impact mood, memory and cognition in a significant subset of women (Epperson et al., 1999; Heikkinen et al., 2006; Joffe and Cohen, 1998; Kugaya et al., 2003; Schmidt et al., 2004; Sherwin, 1991; Soares et al., 2003). We have reported that E±P increased serotonin neural function at multiple levels including gene and protein expression, as well as increased cellular resilience (Bethea et al., 2002; Bethea et al., 2009; Lima and Bethea, 2010). In addition, we have shown that ovariectomized (Ovx) monkeys in a semi-free ranging troop exhibit an increase in anxiety-related behaviors compared to tubal-ligated females, which correlated with a significant decrease in serotonin-related gene expression and neuron number (Bethea et al., 2011; Coleman et al., 2011). These data suggest that the interaction of E, P and serotonin signaling plays a critical role in maintenance of normal affective behavior in primates.

The basic structural unit of neuronal plasticity in the adult nervous system is the dendritic spine (Ethell and Pasquale, 2005), and dendritic spines represent the morphological basis for excitatory neurotransmission (Butler et al., 1998; McKinney et al., 1999). It has been suggested that antidepressants act by promoting neuronal plasticity (Manji et al., 2003). However, E-induced spinogenesis has been explored to a greater extent. In the rodent hippocampus, E±P increase spinogenesis and excitatory glutamatergic input (Gould et al., 1990; Murphy et al., 1998; Woolley and McEwen, 1992). In both the rodent and primate hippocampus, E increases expression of spinogenetic proteins, such as spinophilin, Ras homolog gene family member A (RhoA), and postsynaptic density-95 (PSD-95) (Akama and McEwen, 2003; Brake et al., 2001; Choi et al., 2003; Hao et al., 2003; Kramar et al., 2009; Liu et al., 2008; Spencer et al., 2008; Waters et al., 2009). E±P-induced spinogenesis is also evident, though less studied, in the hypothalamus, amygdala, cerebellum and cortex (de Castilhos et al., 2008; Frankfurt et al., 1990; Hao et al., 2006; Sasahara et al., 2007). We questioned whether E±P-induced spinogenesis also occurs in the dorsal raphe nucleus, where approximately 60% of forebrain serotonergic neurons originate (Jacobs and Azmitia, 1992).

The issue of E and P-induced spinogenesis on serotonin neurons may be important for menopausal women grappling with issues surrounding hormone therapy (HT), which is defined as the administration of E and P to treat deficiencies following menopause. Women experience ovarian failure and loss of E and P production around 50 years of age. Thus, with modern life spans, a woman may live 35–40 years without E and P. We speculate that dendritic spines on serotonin neurons shrink or atrophy due to lack of E and P supported gene and protein expression, which may decrease serotonergic support of higher neural functions. Furthermore, we hypothesize that E and P enhance serotonin neuronal plasticity by increasing spinogenesis on serotonin dendrites, which would facilitate excitatory glutamatergic input to serotonin neurons and in turn, increase serotonin neuronal activity throughout the brain. Maintenance of serotonergic function would support mood, cognition, and circadian rhythms.

Dendritic spine protrusion, maturation and stabilization involve a complex repertoire of cytoskeletal reorganization, expression of glutamate receptors and synapse assembly. We recently found that E±P administration significantly increased gene and protein expression of RhoGTPases and downstream effectors of actin reorganization, increased gene expression for glutamate receptors and increased gene expression for synapse assembly proteins in

serotonin neurons (Bethea and Reddy, 2010; Bethea and Reddy, 2012a; Bethea and Reddy, 2012b; Rivera and Bethea, 2012). We further initiated a study that preliminarily suggested E, P and E+P increased the protein expression of the spine marker protein, PSD-95 (Rivera and Bethea, 2012). This study extends the preliminary study with a statistically significant number of monkeys. We also sought evidence that the increases observed in these spinogenetic molecules translate to changes in the morphology of dorsal raphe spines.

We used a cost effective model of surgical menopause and hormone therapy in which adult rhesus monkeys are Ovx for a relatively short period of time followed by subcutaneous delivery of E and P for 1 month. Therefore, only one time point was examined. We hypothesized that E and P would cause a significant increase in spine maturity and stabilization, which were shown to occur by 24 hours after spine protrusion in the rodent hippocampus (De Roo et al., 2008). In short-term Ovx monkeys, (1) the effect of placebo, E, P, or E+P administration on spinogenesis was determined with immunogold silver staining for PSD-95, and (2) the effect of placebo, E or E+P administration on the morphology of dorsal raphe neurons was determined with Golgi staining.

## Materials and Methods

This experiment was approved by the IACUC of the Oregon National Primate Research Center and conducted in accordance with the 2011 Eighth Edition of the National Institute of Health Guide for the Care and Use of Laboratory Animals. The minimum number of animals to obtain sufficient statistical power was used. Pain was eliminated with anesthetics and analgesics as dictated by the American Veterinary Association and the Animal Welfare Act.

### Animals and E and P treatment

Adult female rhesus monkeys (*Macaca mulatta*) were Ovx 5.7±0.46 months before assignment to this project. Ovariectomy (Ovx) was performed by the surgical personnel of ONPRC according to accepted veterinary surgical protocol. The animals were adult, aged between 5 and 14 years, born in China or USA, weighed between 4 and 11 kg, and were in good health. ONPRC operates with a lease for fee arrangement. Thus, animals had been previously used in select reproductive protocols that had culminated in Ovx before their return to the available pool. The animals had been Ovx after egg and granulosa cell retrieval by laparoscopy, or were Ovx for follicle retrieval and 3D culture. They were rested for at least 5 months between Ovx and assignment to this study.

Ovx monkeys received an empty placebo implant for 28 days (Ovx), an E-filled implant for 28 days (E), a P-filled implant for the final 14 of the 28 days (P) or E for 28 days supplemented with P for the final 14 of the 28 days (E+P). The placebo-treated monkeys received empty Silastic implants (s.c.) on day 0. The E-treated monkeys received one 4.5-cm Silastic implant (i.d. 0.132 in; o.d. 0.183 in; Dow Corning, Midland, MI, USA) filled with crystalline E [1,3,5(10)-estratrien-3, 17B-diol; Steraloids, Wilton, NH, USA] on day 0. The P-treated monkeys received one 6-cm Silastic implant filled with crystalline P (4-pregnen-3, 20-dione; Steraloids) on day 14. The E+P-treated monkeys received one E-filled implant on day 0 and one P-filled capsule on day 14. All implants were placed in the periscapular area under ketamine anesthesia (ketamine hydrochloride, 10 mg/kg s.c.; Fort Dodge Laboratories, Fort Dodge, IA, USA). The E+P treatment regimen has been shown to cause differentiation of the uterine endometrium in a manner similar to the normal 28-day menstrual cycle (Brenner and Slayden, 1994). Animals administered placebo, E, P and E+P were included in the PSD-95 study (n=3/group). Additional animals administered placebo, E and E+P were included in the Golgi study (n=3–4/group). It is important to note that the animals were processed in sets containing 1 animal of each treatment group. This enables a

statistical analysis that corrects for matched sets processed together, but at spaced time intervals for each set.

### Euthanasia

Monkeys were euthanized at the end of the treatment periods according to procedures recommended by the Panel on Euthanasia of the American Veterinary Association. Each animal was sedated with ketamine in the home cage, transported to the necropsy suite, given an overdose of pentobarbital (25 mg/kg i.v., Hospira, Lake Forest, IL, USA) and exsanguinated by severance of the descending aorta.

### Tissue preparation for PSD-95

In the PSD-95 study, the left ventricle of the heart was cannulated and the head of each animal was perfused with 1L of saline followed by 7 L of 4% paraformaldehyde in 3.8% borate, pH 9.5 (both solutions made with 0.1% diethyl pyrocarbonate-treated water to minimize RNase contamination). The brain was removed and dissected. Tissue blocks were post-fixed in 4% paraformaldehyde for 3 h, then transferred to 0.02 M potassium phosphate-buffered saline containing 10% glycerol, followed by 20% glycerol, and 2% dimethyl sulfoxide at 4°C for 3 days to cryoprotect the tissue. After infiltration, the block was frozen in isopentane, cooled to –55°C and stored at –80°C until sectioning. Coronal tissue sections (25 μm) were cut on a sliding microtome, collected in a cryprotectant buffer [30% ethylene glycol and 20% glycerol in 0.05 M sodium phosphate-buffered saline (PBS)], and frozen at –20°C. When tissue sections were ready to be processed they were removed from –20°C storage and washed in 0.01 M PBS (pH 7.4) for 1 h.

### Tissue preparation for Golgi

In the Golgi study, the left ventricle of the heart was cannulated and the head of each animal was perfused with 1.5 L of 0.9 % saline pre-cooled to 4°C. Brains were not perfused with paraformaldehyde because this procedure increases glia staining (Ranjan and Mallick, 2012) making it difficult to isolate neurons for tracing. The brain was removed and dissected.

### PSD-95 immunogold silver staining

Tissue sections first underwent protease section pretreatment adapted from a previous study (Fukaya and Watanabe, 2000). Briefly, a tube containing 0.2 N hydrochloric acid (HCl) was warmed to 37°C in a water bath. Frozen aliquots containing 4 mg/ml of pepsin solution (DAKO, Carpinteria, CA, USA; Catalog No. S3002) were thawed and diluted to 1 mg/ml by adding warm HCl. Tissue sections that had been pre-warmed to 37°C in $H_2O$ were transferred to the 1-mg/ml pepsin solution. After 3 min in pepsin solution, tissue sections were washed in 0.01 M PBS (pH 7.4) for 1 h at RT before being processed with immunogold silver-staining protocol. The immunogold silver-staining protocol used here was adapted from a previous study (Hao et al., 2003). Tissue sections were rinsed in PBS for 10 min, 0.3% Triton for 1 h and blocked with a blocking solution (0.3% Triton, 0.1% cold water fish skin gelatin (Electron Microscopy Sciences, Hatfield, PA, USA; Catalog No. 25560), 0.5% bovine serum albumin (Sigma, St. Louis, MO, USA) and 5% normal goat serum (Vector Laboratories, Burlingame, CA, USA)) for 1 h. Tissue sections were then incubated with primary antibody to PSD-95 for 72 h at 4°C. The PSD-95 polyclonal antibody was raised in rabbit against the *N*-terminal of the mouse peptide (Abcam, Cambridge, MA, USA; Catalog No. ab18258). The PSD-95 antibody was diluted to 1:1,000 in blocking solution. Proper controls for testing specificity of the PSD-95 antibody were previously conducted (Rivera and Bethea, 2012).

After 72 h, tissue sections were washed in PBS for 1 h, an ultra small gold-conjugated goat anti-rabbit antibody (Electron Microscopy Sciences; Catalog No. 25100) diluted to 1:100 in blocking buffer was placed on tissue and incubated for 3 h at RT. After another 1-h PBS wash, tissue sections were post-fixed in 2% glutaraldehyde (Sigma) dissolved in PBS for 10 min, washed in PBS for 2 min, briefly rinsed in $H_2O$ and washed in $H_2O$ for 1 hr. Silver enhancement from Aurion R-Gent-LM kit was used to amplify immunosignal (Electron Microscopy Sciences; Catalog No. 25520). Tissue sections were incubated in silver enhancement solution (18–22°C) for 11 min, washed in $H_2O$ for 15 min and in PBS for 2 min. Tissue sections were mounted onto 2% gelatin-subbed microscope slides and vacuum-dried overnight. The following day, tissue sections were dehydrated with a graded series of ethanols, cleared with Histoclear and coverslipped in Biomount mountant (Electron Microscopy Sciences; Catalog No. 17894).

## Golgi staining

Midbrain tissue blocks were processed using a modified version of the Golgi-Cox method according to manufacturer's protocol (FD Rapid GolgiStain kit PK401, FD Neurotechnologies, Inc., Columbia, MD, USA). This is a two-step procedure to impregnate the tissue block with a chromating solution and to label neurons by immersion in an ammonia solution that forms a mercury-based precipitate. Briefly, tissue blocks were immersed into equal parts Solutions A and B (potassium chromate, potassium dichromate and mercuric chloride) and stored in the dark for 12 d. Tissue blocks were transferred to Solution C and stored in the dark at 4°C for 5 d. After immersion, the block was frozen in isopentane, cooled to –55°C and stored at –80°C until sectioning. Coronal tissue sections (100 μm) were cut on a cryostat, thaw-mounted onto 3% gelatin-subbed microscope slides, vacuum-dried overnight in the dark. The following day, tissue sections were washed in $H_2O$ for 4 min, stained with an ammonia solution composed of Solution D, Solution E and $H_2O$ (1:1:2 ratio) for 10 min, washed in $H_2O$ for 8 min, counterstained with 0.1% Thionin for 4 min, dehydrated in a graded series of ethanols, cleared with Xylene and coverslipped in DPX (Electron Microscopy Sciences).

## PSD-95 stereological analysis

A series of sections at 500-μm intervals through the entire rostro-caudal extent of the dorsal raphe of each monkey was used. The analyses were conducted with a Zeiss Axioplan microscope and StereoInvestigator software (MicroBrightField, Williston, VT, USA). The probe used to estimate total number of PSD-95-positive puncta in the dorsal raphe was the optical fractionator as previously described and used in West et al. (1991) and Hao et al. (2003). It is an unbiased estimate of the total number of PSD-95 puncta in the dorsal raphe obtained by sampling (via systematic random sampling) a fraction of the dorsal raphe. On each tissue section, the operator outlined the dorsal raphe with a 2.5x objective. StereoInvestigator placed counting frames uniformly across a grid containing the dorsal raphe. Counting frame dimensions were 3-μm width and 3-μm height. Grid size dimensions were 250-μm width and 150-μm height. Approximately 73 imaging sites were visited per dorsal raphe outline. For counting of PSD-95-positive puncta, the operator switched the objective to an oil-immersion 100x objective with a high numerical aperture of 1.3. Counting was conducted through an optical dissector height of 3 μm. Guard zone was set at 1 μm. A puncta was counted if it was partly or fully located within inclusion box and as long as it did not touch exclusion lines. We used the estimated population with number weighted section thickness obtained from StereoInvestigator for further analysis. The average tissue thickness was 6 μm and Schmitz Hoff coefficient of error was 0.057.

## Golgi stereological analysis

A series of 8 sections through the dorsal raphe were used for tracing. Tissues sections were coded and measurements were conducted by an experimenter blind to the experimental conditions. A total of 80 neurons were reconstructed in 3D using a Zeiss Axioplan microscope with a blue filter and Neurolucida v9 software (MicroBrightField). On each tissue section, the operator outlined the cell body and dendrites of neurons with a 40x objective. The criteria for inclusion of neurons in analysis were: a) located within the dorsal raphe; b) cell bodies and dendritic tree were entirely stained; c) were relatively isolated from other neurons; and d) contained no beading along branches of dendrites. For counting of dendritic spines, the operator switched the objective to an oil-immersion 100x objective. Counting of each spine was conducted manually throughout dendrites.

NeuroExplorer (MicroBrightField) was then used for analysis of dorsal raphe spine measurements (total spine number and branch order analysis of spine number, dendritic length and spine density). Dorsal raphe cell and dendritic arbor measurements (cell soma size, total dendritic length and total branch number) and dendritic arborization (Sholl analysis with radial unit distances of 10 $\mu$m) were also analyzed.

After the initial analysis, we sampled small sections of higher-order dendrites to determine whether E and P treatment also altered prevalence of 3 spine subtypes (stubby, thin or mushroom) (Sorra and Harris, 2000; Yuste and Bonhoeffer, 2004). Image stacks were captured using the Zeiss brightfield microscope with an oil immersion 100x objective and Neurolucida software. The distance between each image was 0.5 $\mu$m. Image stacks were transformed with Image J (converted to 8-bit, cropped, inverted and contrast was increased) and imported to NeuronStudio software where they were classified into 1 of the 3 spine subtypes (Dumitriu et al., 2011; Rodriguez et al., 2008). Neck ratio was set at 1.1, thin ratio was set at 2.5 and mushroom size was set at 0.35 $\mu$m. A total of 30–49 dendritic sections were sampled from 11–12 neurons per group. Percentages of spines were calculated by totaling the number of each spine and dividing the total number of spines counted and multiplying by 100.

## Photomicrographs and Statistical analysis

Photomicrographs of PSD-95 and Golgi were obtained with a Zeiss Axioplan microscope. PSD-95 photomicrograph images were also converted to binary images with Image J. Also shown are a Sholl analysis that was conducted on a dorsal raphe neuron with NeuroExplorer.

The number of puncta for PSD-95 was totaled for 4 anatomical levels, generating one overall total per monkey. Tissue for PSD-95 was processed in 3 different sets containing 1 animal of each treatment group. Sets 1 and 2 were conducted simultaneously, whereas Set 3 was conducted a year later when additional animals were obtained. Because inter-run variables led to systemic differences in the range of PSD-95 puncta found between sets, the total number of PSD-95 was also expressed as the relative percent change from the Ovx group. The relative percent change from the Ovx group was obtained by subtracting the Ovx value from the E, P or E+P value, dividing by the Ovx value, and multiplying by 100.

All dorsal raphe spines, cell and dendritic arbor measurements were averaged for 8 neurons generating one overall average per monkey.

The mean±SEM in each E, P or E+P treatment group was then obtained for statistical analysis. PSD-95 was analyzed with one-way repeated (matched)-measures ANOVA. Dorsal raphe total spine number, cell soma size, total branch number and total spine number were analyzed with one-way ANOVAs. Branch order analyses and Sholl analysis were analyzed with two-way repeated (matched)-measures ANOVAs. Any significant group

differences (P<0.05) were followed by Newman–Keul's or Bonferonni post hoc tests. Prevalence of spine subtypes in the combined E and E+P groups relative to Ovx group were analyzed with unpaired t-tests. All statistical analyses were conducted using Prism v5.0 software (Graph-Pad, San Diego, CA, USA).

### Ovarian E and P assays

Assays for E and P were performed using Cobas e411 automatic clinical platform (Roche Diagnostics, Indianapolis, IN, USA). Before these analyses, measurements of E and P were compared with traditional radioimmunoassay as previously reported (Bethea et al., 2005).

## Results

### Effect of E and P treatment on dorsal raphe expression of PSD-95 immunogold staining

Representative images of PSD-95-postive puncta in E and P-treated monkeys are shown in Figure 1. There was robust expression of PSD-95-positive puncta in E, P and E+P treated groups, compared to the Ovx-placebo group. The total number of PSD-95-positive puncta in Ovx monkeys treated with placebo, E, P or E+P is shown in Table 1. There was a significant difference between groups in the total number of puncta (ANOVA for matched samples, P=0.0438). E, P and E+P increased the total number of puncta relative to Ovx group (Newman–Keul's, P<0.05 all). Due to a gap in time between processing the 3 sets of monkeys, there were differences in the range of PSD-95 puncta between sets. Therefore, the total number of PSD-95 was also expressed as the relative percent change from the Ovx group in Table 2. There was a significant difference between groups in the relative percent change from the Ovx group (ANOVA, P=0.0410). E, P and E+P treatments increased the relative percent change in comparison to the Ovx group (Newman–Keul's, P<0.05 all).

### Effect of E and P treatment on dorsal raphe dendritic spines

The most prominent neuron types in the dorsal raphe were multipolar and bipolar neurons. Representative images of these neuron types are shown in Figure 2. Both neuron types were used in our analysis (84% of neurons were multipolar; 16% of neurons were bipolar).

There was no difference between the groups in total spine number summed over all branches (ANOVA, P=0.45). However, examination of spines as a function of branch order was revealing. The branch order analysis for dendritic spine number, dendritic length and spine density are shown in Figure 3. There was a significant difference in spine density that depended on branch order (two-way ANOVA, $F_{(2,14)}=7.495$). The E+P treatment significantly increased spine density in higher-order (3–5°) dendritic branches relative to Ovx group (Bonferroni, P<0.05). A representative image of this E+P-induced increase in spine density is shown in Figure 4. This E+P-induced increase in spine density on higher-order dendrites was primarily due to an increase in spine number but no change in dendritic length.

Representative images of 3 spine subtypes (stubby, thin or mushroom) located on higher-order dendritic branches of dorsal raphe neurons after E or E+P administration are shown in Figure 5. There was no statistical difference between combined E and E+P groups relative to the Ovx group on the prevalence of spine subtypes (t-tests, P=0.14–0.83) as shown in Figure 6. Nonetheless, there appears to be a modest trend toward decreased immature thin or filament type spines and increased mature or mushroom type spines after only 1 month of E or E+P administration.

### Effect of E and P treatment on dorsal raphe cell and dendritic arbor

Quantitative analyses of cell and dendritic arbor measurements of cell soma size, total dendritic length and total branch number were conducted and shown in Figure 7. No difference between groups was found in cell soma size, total dendritic length or total branch number (ANOVAs, *Ps*=0.41–0.74).

A representative multipolar neuron from an E+P-treated animal is shown in Figure 2, which was subjected to a Sholl analysis with radial unit distance of 10 μm. The Sholl analysis for overall dendritic arborization was unaffected by E or E+P treatment as shown in Figure 8. As expected, there was a main effect of distance from soma on number of dendritic intersections (ANOVA, P=0.0001). However, there was no difference between groups or interaction (ANOVA, Ps=0.77 and 0.92, respectively).

### Verification of E and P treatment on serum E and P concentrations

Serum was collected at the end of the study to verify the efficacy of Silastic implants. The concentration of E in the serum of E- and E+P-treated groups was 83.2±9 pg/ml and 96.1±13 pg/ml, respectively. The concentration of P in the serum of P- and E+P-treated groups was 7.16±2.24 ng/ml and 3.76±0.63 ng/ml, respectively. The concentrations of E and P are similar to that observed in the mid-luteal phase (Hotchkiss et al., 1982). The concentrations of E and P in the serum of the Ovx group were 15.3±5 pg/ml and 0.05±0.02 ng/ml, respectively (significantly different from E and P-treated monkeys by ANOVAs, *Ps* = 0.0001).

## Discussion

In this report, we show that E, P and E+P increase PSD-95, a pivotal synapse protein, in a statistically significant number of animals. In addition, we found that the increase in expression of PSD-95 by E+P culminates with proliferation of dendritic spines on large serotonin-like neurons of the dorsal raphe.

### E and P regulation of the dorsal raphe spine marker protein, PSD-95

The spinogenetic protein, PSD-95, is a member of the membrane-associated guanylate kinase family. It can bind directly to NMDA receptors or bind indirectly to AMPA receptors (Kornau et al., 1995; Schnell et al., 2002). Moreover, overexpression of PSD-95 promotes spinogenesis (El-Husseini et al., 2000). PSD-95 also regulates the surface expression and synaptic strength of NMDA and AMPA receptors (El-Husseini et al., 2000; Lin et al., 2006; Migaud et al., 1998; Schluter et al., 2006). Therefore, PSD-95 is a positive indicator of synaptic strength as well as a marker protein for dendritic spines.

In the hippocampus and cortex of monkeys, E treatment increased spinophilin, a synaptic scaffold protein and actin-binding regulatory subunit of protein phosphatase 1, as detected with immunogold silver staining and puncta counts. A collaborative study from this laboratory and the McEwen laboratory showed that 1-month of E treatment increased syntaxin, synaptophysin (presynaptic), and spinophilin (postsynaptic) levels in the stratum oriens and radiatum of the CA1 region, and P treatment alone significantly increased synaptophysin levels in the stratum oriens and radiatum of the CA1 region in a manner similar to PSD-95 in the dorsal raphe. Curiously and unlike the raphe, E+P treatment was not different from Ovx-placebo in the hippocampus (Choi et al., 2003). This observation may need confirmation with more animals. PSD-95 protein expression is increased in the hippocampus during proestrus in intact mice and after E treatment in Ovx mice and rats (Li et al., 2004; Spencer et al., 2008; Waters et al., 2009) supporting the notion that PSD-95

induction may be a basic and generalized effect of E and P when the cognate receptors are present.

## E and P regulation of dorsal raphe spine density

The E+P-induced increase in spinogenetic proteins in the dorsal raphe was further translated into a morphological increase in spines. One month of E+P treatment increased spine density in the dorsal raphe on the highest-order dendritic branches. Previous studies of prefrontal cortex showed an increase in spine density in both proximal and distal branches and an increase in the prevalence of thin-type spines, albeit, after a much longer period of E treatment (2–3 years) in young and aged monkeys (Hao et al., 2007; Hao et al., 2006). This may suggest that spine proliferation starts at the furthest reaches of dendrites and that longer E treatment may move the proliferation toward the soma. Although the E+P-induced increase in spine density occurred on more distal dendritic branches, we did not detect any changes in the prevalence of spine subtypes. However, we only examined spine changes after 1 month of treatment. Perhaps a longer period of treatment would have lead to more robust changes in spine morphology.

Temporal efficacy may differ between species. In Ovx monkeys, 1 month and 2–3 years of E treatment has been reported to increase spines (Leranth et al., 2002; Hao et al., 2006; Hao et al., 2007). However, a much shorter duration of E (ranging from 48–72h) is reported to increase spines in rodents (Gould et al., 1990; Woolley and McEwen, 1992). One might speculate that length of E treatment required to increase spines is reflective of the length of their reproductive cycle. Unlike rodents, nonhuman primates have a menstrual cycle that lasts for 28 days and they reach puberty around 3 years of age. Rodents reach puberty in days rather than years, and they have a much shorter life span and higher metabolism than primates. Thus, it is not entirely surprising that E acts faster in the rodent brain than primate brain.

## Mechanism of Action of E and P

Serotonin neurons contain estrogen receptor subtype β (ERβ) and administration of E causes an induction of nuclear progesterone receptor (PR), which is maintained during supplemental P (Bethea, 1993; Bethea, 1994; Gundlah et al., 2001). However in the absence of E, there is little or no nuclear PR expression. In serotonin neurons, the action of P alone varies with the endpoint examined and there is no solid explanation. For example, P alone increased TPH-2 gene expression and $^{3}$H-citalopram ligand binding in a manner similar to E (Lu et al., 2003; Sanchez et al., 2005); P alone decreased $5HT_{1A}$ receptor binding and MAO-A gene expression in a manner similar to E (Gundlah et al., 2002; Lu and Bethea, 2002), but P alone was not different from the Ovx-placebo group with regard to NFkB translocation (Bethea et al., 2006).

P alone increased the expression of the spine marker protein, PSD-95. Furthermore, E+P treatment was similar to treatment with E alone or P alone on these parameters, showing neither an attenuating nor a potentiating effect. The stimulatory effect of P alone on PSD-95 may be independent of nuclear PR, mediated instead by an indirect or nongenomic action of P. When P is converted to its active metabolite, allopregnanolone, it can act through the gamma-aminobutyric acid receptor subtype A ($GABA_A$) (Majewska et al., 1986). GABA is generally considered inhibitory, therefore, this scenario invokes an excitatory interneuron. P may also invoke nongenomic actions by acting on membrane PRs and progesterone receptor membrane component 1 (Zhu et al., 2003; Meyer et al., 1996). In addition, it is noteworthy that E alone stimulated PSD-95 (and nuclear PR expression as previously published), but the addition of P to the E regimen had no further effect. Thus, P treatment was neutral on PSD-95 when added to the E regimen.

P facilitated the effect of E on spine density on higher-order dendritic branches after 1 month of treatment. E may be priming spine formation by increasing the amount of spinogenetic proteins available or by inducing nuclear PR. An additional stimulus, such as added P treatment, then produced a morphological change in spine density in this time frame. We have previously observed this same stimulatory effect of E+P, but not of E alone, on MAPK kinase 5 gene expression in serotonin neurons (Bethea and Reddy, 2008). The effects of E or P independently or in combination in the serotonin system remain enigmatic. We hope that future examination of the promoter regions of responsive genes in serotonin neurons will advance our comprehension of the mechanisms of action of E and P in this important system.

### Comparison of PSD-95 and Dendritic Spines

The induction of PSD-95 by E in the monkey raphe is consistent with previous observations in other brain areas. However, our data on PSD-95 does not closely follow the morphological increase in spines. There was no statistical difference in spines between E alone and the Ovx group. However, there was no difference in spines between E alone and E +P either. The sampling of changes in gene and protein expression of RhoGTPases, synapse assembly proteins and glutamate receptors in serotonin neurons (thousands of cells with laser-capture and microarray, hundreds of cells with ICC) and the sampling of Golgi-labeled spines is different by an order of magnitude or more. In this study, the increase in spines with E treatment was not statistically higher than Ovx or statistically lower than E+P. The SEM around spine density in the E treated group is large and hinders statistical analysis. It may be that a longer treatment time, greater sampling of higher-order dendritic branches, or more monkeys, would have revealed an increase with E treatment. Since PSD-95 increased with E alone, and PSD-95 is a spine marker protein, it is likely that this is a type 2 statistical-error, due to small numbers of subjects.

### Translational relevance

What does the loss of dendritic spines on serotonin neurons mean for women after menopause and how long would it take for symptoms to manifest? The loss of spines means a loss of stimulatory glutamatergic input to the serotonin system. This would result in less serotonin neurotransmission to forebrain areas supporting mood, memory and executive function. Our data and that of others suggest that in women, correct formulations of hormone therapy may be an important intervention. For women who cannot use estrogenic compounds, further advances are necessary. Research conducted in the hippocampus and prefrontal cortex reveals that physical and mental exercise can help retain neural function by maintaining dendritic spines (Stranahan et al., 2007; Leuner et al., 2003).

### Conclusion

A combination of E+P leads to the elaboration of dendritic spines on dorsal raphe neurons in short-term Ovx monkeys after 1 month of treatment. Increased spinogenesis on serotonin neurons would improve numerous mental health parameters. The ability of E to induce PSD-95 and other pivotal spinogenetic genes and proteins, but not actual spines after 1 month, suggests either a sampling issue or a time lag issue. The effect of hormone therapy on spine density after a long absence is of significant interest and animals are being prepared to study this issue in greater detail.

## Acknowledgments

## References

Akama KT, McEwen BS. Estrogen stimulates postsynaptic density-95 rapid protein synthesis via the Akt/protein kinase B pathway. J Neurosci. 2003; 23(6):2333–2339. [PubMed: 12657692]

Bethea CL. Colocalization of progestin receptors with serotonin in raphe neurons of macaque. Neuroendocrinology. 1993; 57(1):1–6. [PubMed: 8479605]

Bethea CL. Regulation of progestin receptors in raphe neurons of steroid-treated monkeys. Neuroendocrinology. 1994; 60(1):50–61. [PubMed: 8090282]

Bethea CL, Lu NZ, Gundlah C, Streicher JM. Diverse actions of ovarian steroids in the serotonin neural system. Front Neuroendocrinol. 2002; 23(1):41–100. [PubMed: 11906203]

Bethea CL, Reddy AP. Effect of ovarian hormones on genes promoting dendritic spines in laser-captured serotonin neurons from macaques. Mol Psychiatry. 2010; 15(10):1034–1044. [PubMed: 19687787]

Bethea CL, Reddy AP. Effect of ovarian steroids on gene expression related to synapse assembly in serotonin neurons of macaques. J Neurosci Res. 2012a; 90(7):1324–1334. [PubMed: 22411564]

Bethea CL, Reddy AP. Ovarian steroids increase glutamatergic related gene expression in serotonin neurons of macaques. Mol Cell Neurosci. 2012b; 49(3):251–262. [PubMed: 22154832]

Bethea CL, Reddy AP, Smith LJ. Nuclear factor kappa B in the dorsal raphe of macaques: an anatomical link for steroids, cytokines and serotonin. Journal of psychiatry & neuroscience : JPN. 2006; 31(2):105–114. [PubMed: 16575426]

Bethea CL, Reddy AP, Tokuyama Y, Henderson JA, Lima FB. Protective actions of ovarian hormones in the serotonin system of macaques. Front Neuroendocrinol. 2009; 30(2):212–238. [PubMed: 19394356]

Bethea CL, Smith AW, Centeno ML, Reddy AP. Long-term ovariectomy decreases serotonin neuron number and gene expression in free ranging macaques. Neuroscience. 2011

Bethea CL, Streicher JM, Mirkes SJ, Sanchez RL, Reddy AP, Cameron JL. Serotonin-related gene expression in female monkeys with individual sensitivity to stress. Neuroscience. 2005; 132(1): 151–166. [PubMed: 15780474]

Bethea CL, Reddy AP. Effect of ovarian hormones on survival genes in laser captured serotonin neurons from macaques. J Neurochem. 2008; 105(4):1129–1143. [PubMed: 18182058]

Brake WG, Alves SE, Dunlop JC, Lee SJ, Bulloch K, Allen PB, Greengard P, McEwen BS. Novel target sites for estrogen action in the dorsal hippocampus: an examination of synaptic proteins. Endocrinology. 2001; 142(3):1284–1289. [PubMed: 11181546]

Brenner RM, Slayden OD. Oestrogen action in the endometrium and oviduct of rhesus monkeys during RU486 treatment. Hum Reprod. 1994; 9(Suppl 1):82–97. [PubMed: 7962475]

Butler AK, Uryu K, Chesselet MF. A role for N-methyl-D-aspartate receptors in the regulation of synaptogenesis and expression of the polysialylated form of the neural cell adhesion molecule in the developing striatum. Dev Neurosci. 1998; 20(2–3):253–262. [PubMed: 9691199]

Choi JM, Romeo RD, Brake WG, Bethea CL, Rosenwaks Z, McEwen BS. Estradiol increases pre- and post-synaptic proteins in the CA1 region of the hippocampus in female rhesus macaques (Macaca mulatta). Endocrinology. 2003; 144(11):4734–4738. [PubMed: 12960039]

Coleman K, Robertson ND, Bethea CL. Long-term ovariectomy alters social and anxious behaviors in semi-free ranging Japanese macaques. Behav Brain Res. 2011; 225(1):317–327. [PubMed: 21835209]

de Castilhos J, Forti CD, Achaval M, Rasia-Filho AA. Dendritic spine density of posterodorsal medial amygdala neurons can be affected by gonadectomy and sex steroid manipulations in adult rats: a Golgi study. Brain Res. 2008; 1240:73–81. [PubMed: 18809393]

De Roo M, Klauser P, Muller D. LTP promotes a selective long-term stabilization and clustering of dendritic spines. PLoS Biol. 2008; 6(9):e219. [PubMed: 18788894]

Dumitriu D, Rodriguez A, Morrison JH. High-throughput, detailed, cell-specific neuroanatomy of dendritic spines using microinjection and confocal microscopy. Nature protocols. 2011; 6(9): 1391–1411.

El-Husseini AE, Schnell E, Chetkovich DM, Nicoll RA, Bredt DS. PSD-95 involvement in maturation of excitatory synapses. Science. 2000; 290(5495):1364–1368. [PubMed: 11082065]

Epperson CN, Wisner KL, Yamamoto B. Gonadal steroids in the treatment of mood disorders. Psychosom Med. 1999; 61(5):676–697. [PubMed: 10511016]

Ethell IM, Pasquale EB. Molecular mechanisms of dendritic spine development and remodeling. Prog Neurobiol. 2005; 75(3):161–205. [PubMed: 15882774]

Frankfurt M, Gould E, Woolley CS, McEwen BS. Gonadal steroids modify dendritic spine density in ventromedial hypothalamic neurons: a Golgi study in the adult rat. Neuroendocrinology. 1990; 51(5):530–535. [PubMed: 2112730]

Fukaya M, Watanabe M. Improved immunohistochemical detection of postsynaptically located PSD-95/SAP90 protein family by protease section pretreatment: a study in the adult mouse brain. J Comp Neurol. 2000; 426(4):572–586. [PubMed: 11027400]

Gould E, Woolley CS, Frankfurt M, McEwen BS. Gonadal steroids regulate dendritic spine density in hippocampal pyramidal cells in adulthood. J Neurosci. 1990; 10(4):1286–1291. [PubMed: 2329377]

Gundlah C, Lu NZ, Bethea CL. Ovarian steroid regulation of monoamine oxidase-A and -B mRNAs in the macaque dorsal raphe and hypothalamic nuclei. Psychopharmacology (Berl). 2002; 160(3): 271–282. [PubMed: 11889496]

Gundlah C, Lu NZ, Mirkes SJ, Bethea CL. Estrogen receptor beta (ERbeta) mRNA and protein in serotonin neurons of macaques. Brain Res Mol Brain Res. 2001; 91(1–2):14–22. [PubMed: 11457488]

Hao J, Janssen WG, Tang Y, Roberts JA, McKay H, Lasley B, Allen PB, Greengard P, Rapp PR, Kordower JH, Hof PR, Morrison JH. Estrogen increases the number of spinophilin-immunoreactive spines in the hippocampus of young and aged female rhesus monkeys. J Comp Neurol. 2003; 465(4):540–550. [PubMed: 12975814]

Hao J, Rapp PR, Janssen WG, Lou W, Lasley BL, Hof PR, Morrison JH. Interactive effects of age and estrogen on cognition and pyramidal neurons in monkey prefrontal cortex. Proc Natl Acad Sci U S A. 2007; 104(27):11465–11470. [PubMed: 17592140]

Hao J, Rapp PR, Leffler AE, Leffler SR, Janssen WG, Lou W, McKay H, Roberts JA, Wearne SL, Hof PR, Morrison JH. Estrogen alters spine number and morphology in prefrontal cortex of aged female rhesus monkeys. J Neurosci. 2006; 26(9):2571–2578. [PubMed: 16510735]

Heikkinen J, Vaheri R, Timonen U. A 10-year follow-up of postmenopausal women on long-term continuous combined hormone replacement therapy: Update of safety and quality-of-life findings. J Br Menopause Soc. 2006; 12(3):115–125. [PubMed: 16953985]

Hotchkiss J, Dierschke DJ, Butler WR, Fritz GR, Knobil E. Relation between levels of circulating ovarian steroids and pituitary gonadotropin content during the menstrual cycle of the rhesus monkey. Biol Reprod. 1982; 26(2):241–248. [PubMed: 6802194]

Jacobs BL, Azmitia EC. Structure and function of the brain serotonin system. Physiol Rev. 1992; 72(1):165–229. [PubMed: 1731370]

Joffe H, Cohen LS. Estrogen, serotonin, and mood disturbance: where is the therapeutic bridge? Biol Psychiatry. 1998; 44(9):798–811. [PubMed: 9807636]

Kornau HC, Schenker LT, Kennedy MB, Seeburg PH. Domain interaction between NMDA receptor subunits and the postsynaptic density protein PSD-95. Science. 1995; 269(5231):1737–1740. [PubMed: 7569905]

Kramar EA, Chen LY, Brandon NJ, Rex CS, Liu F, Gall CM, Lynch G. Cytoskeletal changes underlie estrogen's acute effects on synaptic transmission and plasticity. J Neurosci. 2009; 29(41):12982–12993. [PubMed: 19828812]

Kugaya A, Epperson CN, Zoghbi S, van Dyck CH, Hou Y, Fujita M, Staley JK, Garg PK, Seibyl JP, Innis RB. Increase in prefrontal cortex serotonin 2A receptors following estrogen treatment in postmenopausal women. Am J Psychiatry. 2003; 160(8):1522–1524. [PubMed: 12900319]

Leranth C, Shanabrough M, Redmond DE Jr. Gonadal hormones are responsible for maintaining the integrity of spine synapses in the CA1 hippocampal subfield of female nonhuman primates. J Comp Neurol. 2002; 447(1):34–42. [PubMed: 11967893]

Leuner B, Falduto J, Shors TJ. Associative memory formation increases the observation of dendritic spines in the hippocampus. J Neurosci. 2003; 23(2):659–665. [PubMed: 12533625]

Li C, Brake WG, Romeo RD, Dunlop JC, Gordon M, Buzescu R, Magarinos AM, Allen PB, Greengard P, Luine V, McEwen BS. Estrogen alters hippocampal dendritic spine shape and enhances synaptic protein immunoreactivity and spatial memory in female mice. Proc Natl Acad Sci U S A. 2004; 101(7):2185–2190. [PubMed: 14766964]

Lima FB, Bethea CL. Ovarian steroids decrease DNA fragmentation in the serotonin neurons of non-injured rhesus macaques. Mol Psychiatry. 2010; 15(6):657–668. [PubMed: 19823180]

Lin Y, Jover-Mengual T, Wong J, Bennett MV, Zukin RS. PSD-95 and PKC converge in regulating NMDA receptor trafficking and gating. Proc Natl Acad Sci U S A. 2006; 103(52):19902–19907. [PubMed: 17179037]

Liu F, Day M, Muniz LC, Bitran D, Arias R, Revilla-Sanchez R, Grauer S, Zhang G, Kelley C, Pulito V, Sung A, Mervis RF, Navarra R, Hirst WD, Reinhart PH, Marquis KL, Moss SJ, Pangalos MN, Brandon NJ. Activation of estrogen receptor-beta regulates hippocampal synaptic plasticity and improves memory. Nat Neurosci. 2008; 11(3):334–343. [PubMed: 18297067]

Lu NZ, Bethea CL. Ovarian steroid regulation of 5-HT1A receptor binding and G protein activation in female monkeys. Neuropsychopharmacology. 2002; 27(1):12–24. [PubMed: 12062903]

Lu NZ, Eshleman AJ, Janowsky A, Bethea CL. Ovarian steroid regulation of serotonin reuptake transporter (SERT) binding, distribution, and function in female macaques. Mol Psychiatry. 2003; 8(3):353–360. [PubMed: 12660809]

Majewska MD, Harrison NL, Schwartz RD, Barker JL, Paul SM. Steroid hormone metabolites are barbiturate-like modulators of the GABA receptor. Science. 1986; 232(4753):1004–1007. [PubMed: 2422758]

Manji HK, Quiroz JA, Sporn J, Payne JL, Denicoff K, NAG, Zarate CA Jr, Charney DS. Enhancing neuronal plasticity and cellular resilience to develop novel, improved therapeutics for difficult-to-treat depression. Biol Psychiatry. 2003; 53(8):707–742. [PubMed: 12706957]

McKinney RA, Capogna M, Durr R, Gahwiler BH, Thompson SM. Miniature synaptic events maintain dendritic spines via AMPA receptor activation. Nat Neurosci. 1999; 2(1):44–49. [PubMed: 10195179]

Meyer C, Schmid R, Scriba PC, Wehling M. Purification and partial sequencing of high-affinity progesterone-binding site(s) from porcine liver membranes. Eur J Biochem. 1996; 239 (3):726–731. [PubMed: 8774719]

Migaud M, Charlesworth P, Dempster M, Webster LC, Watabe AM, Makhinson M, He Y, Ramsay MF, Morris RG, Morrison JH, O'Dell TJ, Grant SG. Enhanced long-term potentiation and impaired learning in mice with mutant postsynaptic density-95 protein. Nature. 1998; 396(6710):433–439. [PubMed: 9853749]

Murphy DD, Cole NB, Segal M. Brain-derived neurotrophic factor mediates estradiol-induced dendritic spine formation in hippocampal neurons. Proc Natl Acad Sci U S A. 1998; 95(19):11412–11417. [PubMed: 9736750]

Ranjan A, Mallick BN. Differential staining of glia and neurons by modified Golgi-Cox method. J Neurosci Methods. 2012; 209(2):269–279. [PubMed: 22750653]

Ressler KJ, Nemeroff CB. Role of serotonergic and noradrenergic systems in the pathophysiology of depression and anxiety disorders. Depress Anxiety. 2000; 12(Suppl 1):2–19. [PubMed: 11098410]

Rivera HM, Bethea CL. Ovarian steroids increase spinogenetic proteins in the macaque dorsal raphe. Neuroscience. 2012; 208:27–40. [PubMed: 22342969]

Rodriguez A, Ehlenberger DB, Dickstein DL, Hof PR, Wearne SL. Automated three-dimensional detection and shape classification of dendritic spines from fluorescence microscopy images. PLoS One. 2008; 3(4):e1997. [PubMed: 18431482]

Sanchez RL, Reddy AP, Centeno ML, Henderson JA, Bethea CL. A second tryptophan hydroxylase isoform, TPH-2 mRNA, is increased by ovarian steroids in the raphe region of macaques. Brain Res Mol Brain Res. 2005; 135(1–2):194–203. [PubMed: 15857682]

Sasahara K, Shikimi H, Haraguchi S, Sakamoto H, Honda S, Harada N, Tsutsui K. Mode of action and functional significance of estrogen-inducing dendritic growth, spinogenesis, and synaptogenesis in the developing Purkinje cell. J Neurosci. 2007; 27(28):7408–7417. [PubMed: 17626201]

Schluter OM, Xu W, Malenka RC. Alternative N-terminal domains of PSD-95 and SAP97 govern activity-dependent regulation of synaptic AMPA receptor function. Neuron. 2006; 51(1):99–111. [PubMed: 16815335]

Schmidt PJ, Haq N, Rubinow DR. A longitudinal evaluation of the relationship between reproductive status and mood in perimenopausal women. Am J Psychiatry. 2004; 161(12):2238–2244. [PubMed: 15569895]

Schnell E, Sizemore M, Karimzadegan S, Chen L, Bredt DS, Nicoll RA. Direct interactions between PSD-95 and stargazin control synaptic AMPA receptor number. Proc Natl Acad Sci U S A. 2002; 99(21):13902–13907. [PubMed: 12359873]

Sherwin BB. The impact of different doses of estrogen and progestin on mood and sexual behavior in postmenopausal women. J Clin Endocrinol Metab. 1991; 72(2):336–343. [PubMed: 1846872]

Soares CN, Poitras JR, Prouty J. Effect of reproductive hormones and selective estrogen receptor modulators on mood during menopause. Drugs Aging. 2003; 20(2):85–100. [PubMed: 12534310]

Sorra KE, Harris KM. Overview on the structure, composition, function, development, and plasticity of hippocampal dendritic spines. Hippocampus. 2000; 10(5):501–511. [PubMed: 11075821]

Spencer JL, Waters EM, Milner TA, McEwen BS. Estrous cycle regulates activation of hippocampal Akt, LIM kinase, and neurotrophin receptors in C57BL/6 mice. Neuroscience. 2008; 155(4):1106–1119. [PubMed: 18601981]

Stranahan AM, Khalil D, Gould E. Running induces widespread structural alterations in the hippocampus and entorhinal cortex. Hippocampus. 2007; 17(11):1017–1022. [PubMed: 17636549]

Waters EM, Mitterling K, Spencer JL, Mazid S, McEwen BS, Milner TA. Estrogen receptor alpha and beta specific agonists regulate expression of synaptic proteins in rat hippocampus. Brain Res. 2009; 1290:1–11. [PubMed: 19596275]

West MJ, Slomianka L, Gundersen HJ. Unbiased stereological estimation of the total number of neurons in thesubdivisions of the rat hippocampus using the optical fractionator. Anat Rec. 1991; 231(4):482–497. [PubMed: 1793176]

Woolley CS, McEwen BS. Estradiol mediates fluctuation in hippocampal synapse density during the estrous cycle in the adult rat. J Neurosci. 1992; 12(7):2549–2554. [PubMed: 1613547]

Yuste R, Bonhoeffer T. Genesis of dendritic spines: insights from ultrastructural and imaging studies. Nat Rev Neurosci. 2004; 5(1):24–34. [PubMed: 14708001]

Zhu Y, Bond J, Thomas P. Identification, classification, and partial characterization of genes in humans and other vertebrates homologous to a fish membrane progestin receptor. Proc Natl Acad Sci U S A. 2003; 100(5):2237–2242. [PubMed: 12601167]
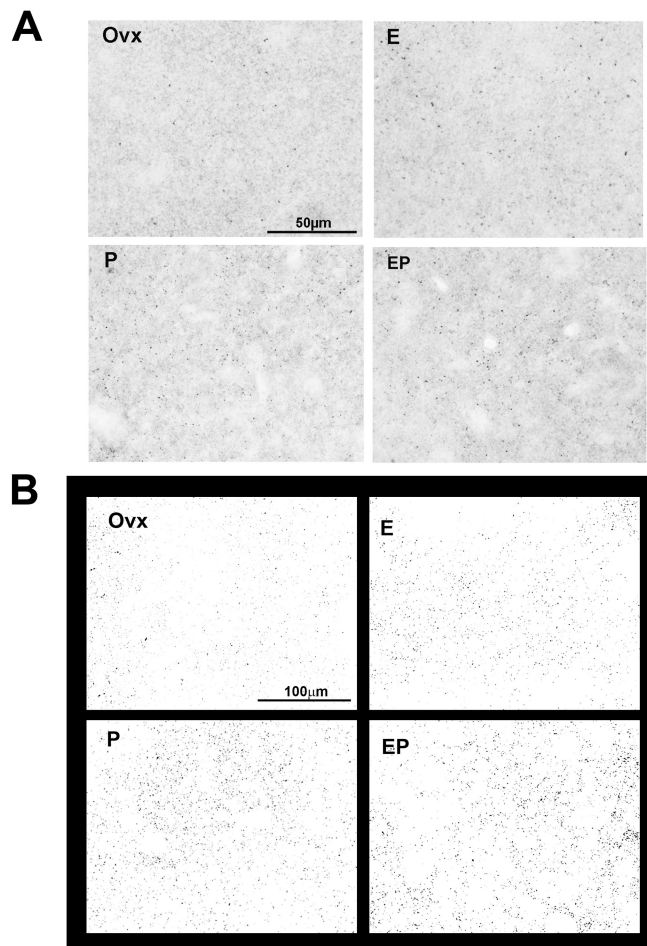
**Figure 1.**
Representative photomicrograph and segmented images of PSD-95-positive puncta in Ovx monkeys treated with placebo, E, P or E+P. (A) Photomicrograph images for PSD-95 were captured with StereoInvestigator at 40X and cropped to a smaller field-of-view. (B) Photomicrograph images captured with a larger field-of-view were converted to binary images using Image J. There was robust expression of PSD-95-positive puncta in E, P and E +P groups, but it was reduced in Ovx group. Scale bar in photomicrograph image = 50 µm. Scale bar in segmented image = 100 µm.
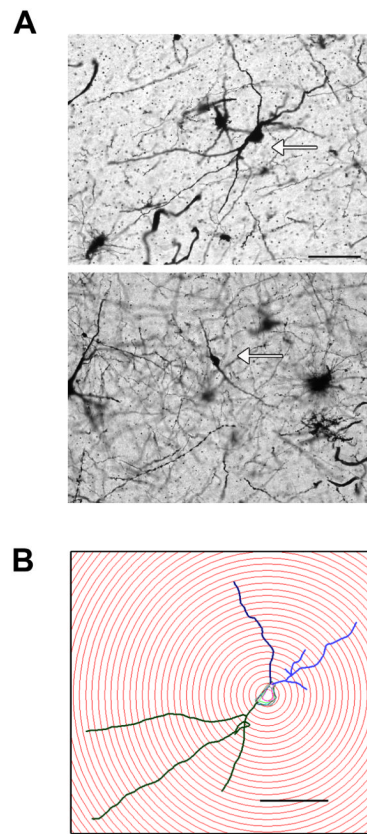
**Figure 2.**
Representative images of neuron types found in dorsal raphe. A) The most prominent neuron types stained with Golgi were multipolar and bipolar neurons (arrows). Both neuron types were used in our analysis (84% of neurons were multipolar; 16% of neurons were bipolar). Scale bar = 100 μm. B) Representative multipolar neuron from an E+P-treated animal subjected to a Sholl analysis. Scale bar = 100 μm.
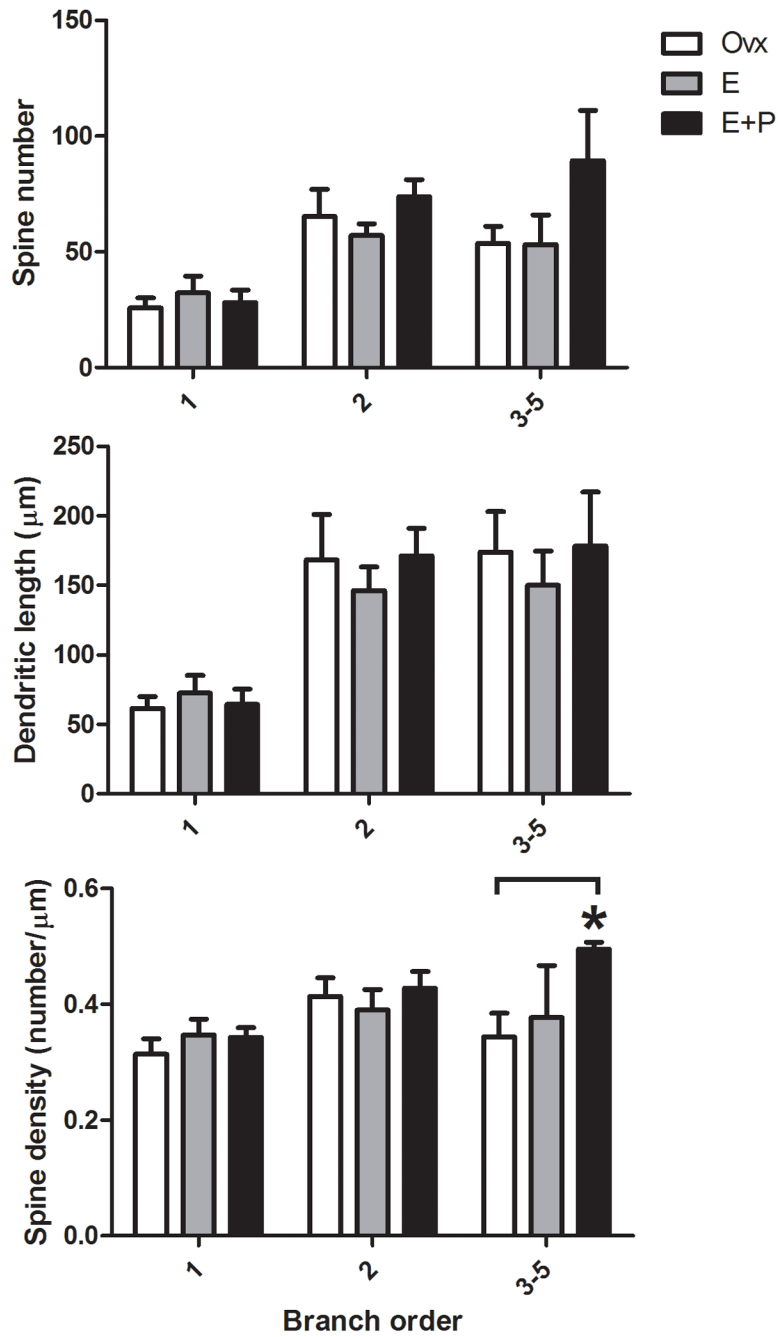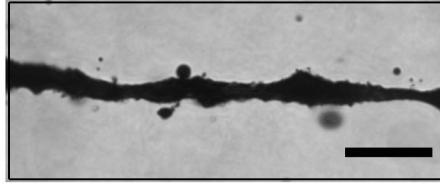
**Figure 3.**
Branch order analysis for dendritic spine number, dendritic length and spine density in the dorsal raphe of Ovx monkeys treated with placebo, E or E+P (n = 3–4/group). There was a significant difference in spine density that depended on branch order (two-way ANOVA, $F_{(2,14)}=7.495$). E+P treatment significantly increased spine density in higher-order (3–5°) dendritic branches relative to Ovx group (Bonferroni, $P<0.05$). This E+P-induced increase in spine density on higher-order dendrites was primarily due to an increase in spine number, but no change in dendritic length. *E+P greater than Ovx with Bonferroni, $P<0.05$.
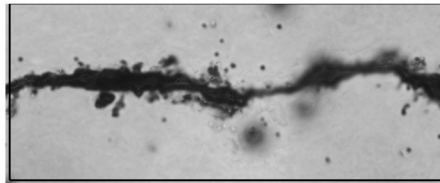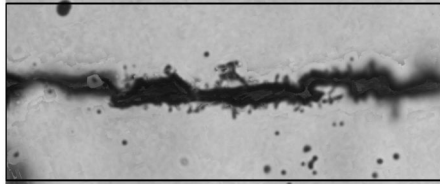
# Ovx



# EP



**Figure 4.**
A representative photomicrograph of E+P-induced increase in spine density in dorsal raphe. Photomicrograph images for dendritic spines were captured with StereoInvestigator at 100X and cropped. There were more dendritic spines in the E+P group relative to the Ovx group. Scale bar in photomicrograph image = 10 μm.
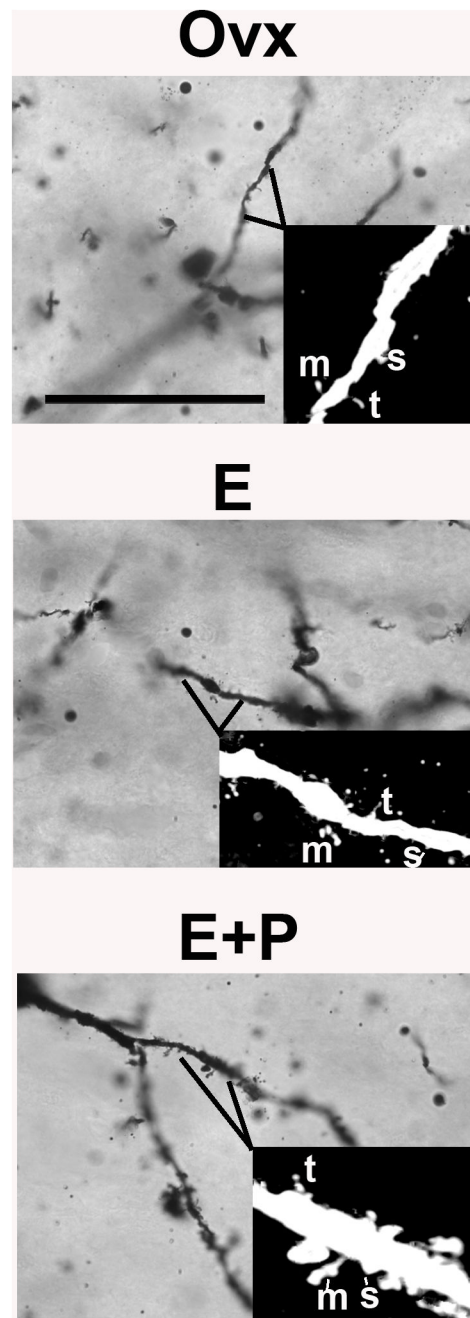


**Figure 5.**
Representative images of 3 spine subtypes (stubby, thin or mushroom) located on higher-order dendritic branches of dorsal raphe neurons in placebo, E or E+P treated monkeys. Image stacks were captured with Neurolucida at 100X. Inset image was further transformed with Image J (converted to 8-bit, cropped, inverted and contrast was increased) and imported to Neuronstudio to analyze spine subtype. Abbreviations, s = stubby, t = thin, m = mushroom. Scale bar in photomicrograph image = 50 μm.
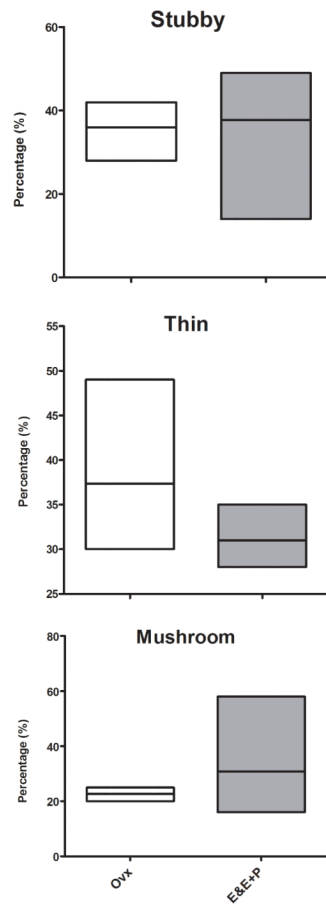
**Figure 6.**
Prevalence of spine subtypes (stubby, thin or mushroom) was not affected by E or E+P treatment. No group difference between combined E and E+P groups relative to the Ovx group was found on the prevalence of spine subtypes (t-tests, P=0.14–0.83) but there appears to be a modest trend toward decreased immature thin or filament type spines and increased mature or mushroom type spines after only 1 month of E or E+P treatment.
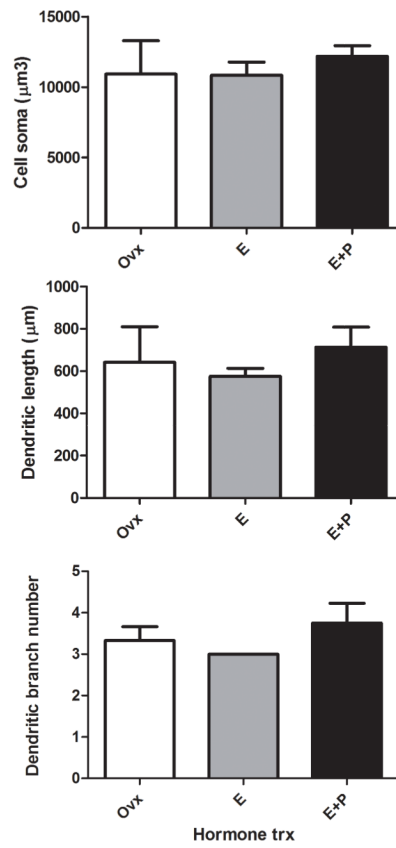
**Figure 7.**
Cell and dendritic arbor measurements of cell soma size, total dendritic length and total branch number were not affected by E or E+P treatment. No group difference was found on cell soma size, total dendritic length or total branch number (ANOVAs, Ps=0.41–0.74).
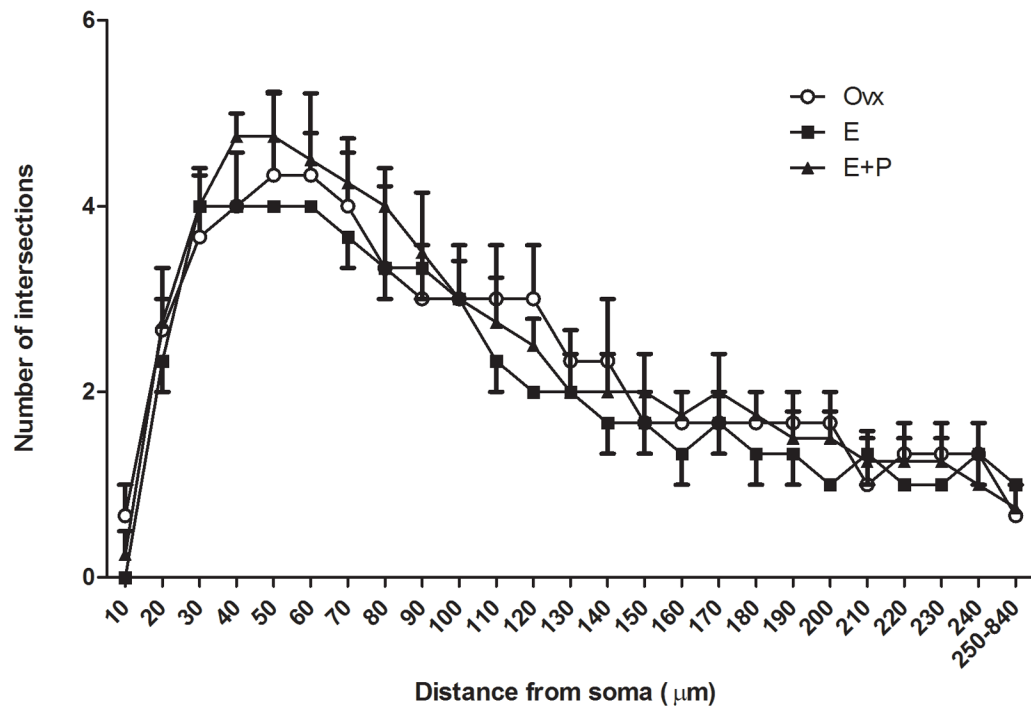
**Figure 8.**
Sholl analysis showed that overall dendritic arborization was not affected by E or E+P treatment. As expected, there was a main effect of distance from soma on number of dendritic intersections (ANOVA, P=0.0001). However, there was no group difference or interaction (ANOVA, Ps=0.77 and 0.92, respectively). For better visibility of means, only top error bars were included for Ovx and E+P groups and only bottom error bars were included for E group.

**Table 1**

The total number of PSD-95-positive puncta in the dorsal raphe of Ovx monkeys treated with placebo, E, P or E+P ($n = 3$/group).

| Set | Ovx | E | P | E+P | F-values |
|---|---|---|---|---|---|
| 1 | 13294133 | 18746336 | 18559261 | 19817792 | |
| 2 | 13621572 | 17031957 | 17718689 | 20687377 | |
| 3 | 6590748 | 8127561 | 9514303 | 7161746 | |
| | **11168818 ± 2290986** | **14635285 ± 3291283**[*] | **15264084 ± 2885113**[*] | **15888972 ± 4370827**[*] | $F(3,11) = 5.08$, $P < 0.05$ |

The number of puncta for PSD-95 was totaled for 4 anatomical levels, generating one overall total per monkey. Tissue for PSD-95 was processed in 3 different sets containing 1 animal of each treatment group. Sets 1 and 2 were conducted simultaneously, whereas Set 3 was conducted a year later when additional monkeys were obtained. Data values in bold are mean±SEM. There was a significant difference between groups in the total number of puncta (ANOVA for matched samples $P = 0.0438$).

[*]
E, P and E+P greater than Ovx with Newman–Keul's, $P<0.05$ all.

**Table 2**

E, P and E+P treatment increased the relative percent change of PSD-95 from the Ovx group ($n = 3$/group).

| Set | Ovx | E | P | E+P | F-values |
|---|---|---|---|---|---|
| 1 | 0 % | 41 % | 40 % | 49 % | |
| 2 | 0 % | 25 % | 30 % | 52 % | |
| 3 | 0 % | 23 % | 44 % | 9 % | |
| | **0 ± 0 %** [*] | **30 ± 6 %** [*] | **38 ± 4 %** [*] | **37 ± 14 %** [*] | $F_{(3,11)} = 5.24$, $P < 0.05$ |

Because inter-run variables led to systemic differences in the range of PSD-95 puncta found between sets, the total number of PSD-95 was also expressed as the relative percent change from the Ovx group. The relative percent change from the Ovx group was obtained by subtracting the Ovx value from the E, P or E+P value, dividing by the Ovx value, and multiplying by 100. Data values in bold are mean ±SEM. There was a significant difference between groups in the relative percent change from the Ovx group (ANOVA, P=0.0410).

[*] E, P and E+P greater than Ovx with Newman–Keul's, P<0.05 all.